Intensity-related dynamics of femtosecond frequency combs

Kevin W. Holman, R. Jason Jones, Adela Marian, Steven T. Cundiff, and Jun Ye

JILA, National Institute of Standards and Technology and University of Colorado, Boulder, Colorado 80309-0440

Received November 13, 2002

We have performed systematic studies of intensity-related dynamics of the pulse repetition and carrier-envelope offset frequencies in mode-locked Ti:sapphire lasers. We compared the results for two laser systems that have different intracavity dispersion-compensation schemes. We found that the carrier-envelope phase noise and its dynamic response depend critically on the mode-locking conditions. An intensity-related shift of the laser spectrum was found to be instrumental in interpretations. © 2003 Optical Society of America

OCIS codes: 320.0320, 140.7090, 140.4050.

Stabilized mode-locked femtosecond lasers have played a key role in the recent advances in optical frequency measurement,[1,2] carrier-envelope phase stabilization,[3,4] optical clocks,[5,6] optical frequency synthesizers,[7] and pulse synthesis.[8] Their many applications provide a strong motivation to develop the ultrafast laser to be more reliable, more stable, and easier to control. Conversely, armed with precision measurement tools, we can also further our understanding of the mode-locking mechanism and dynamics of the laser.

At present, the most versatile and reliable ultrafast lasers are Kerr-lens mode-locked Ti:sapphire (Ti:s) systems. There are two basic configurations that compensate for group-velocity dispersion (GVD). One utilizes an intracavity prism pair, and the other takes advantage of negatively chirped mirrors. The other system facilitates use of a reduced cavity size at the expense of limited fine tuning of the intracavity GVD. Here we use a prism-based laser system with a 100-MHz repetition rate and a prismless laser with a 750-MHz repetition rate. Both laser systems have successfully produced octave-bandwidth optical frequency combs with microstructure fibers. Compared with that of the 100-MHz laser, the reduced energy per pulse in the 750-MHz laser requires a higher average power and (or) an increased nonlinear interaction length for continuum generation. However, the 750-MHz laser is advantageous in heterodyne detection between one of the comb lines and a cw laser. It is also attractive for its easier-to-identify comb mode orders.

The two degrees of freedom associated with the optical comb are the laser repetition frequency ($f_{\rm rep}$) and the carrier-envelope offset frequency ($f_{\rm ceo}$): $f_{\rm rep} = \nu_g/l_c$ and $f_{\rm ceo} = (\omega_c/2\pi)(1 - \nu_g/\nu_p)$, where ω_c is the pulse carrier frequency, l_c is the cavity length, and ν_g (ν_p) is the average group (phase) velocity inside the cavity.[9] The absolute frequency of each comb line is given by $f_m = mf_{\rm rep} + f_{\rm ceo}$. In the time domain the pulse-to-pulse carrier-envelope phase shift is expressed as $\Delta\phi = 2\pi f_{\rm ceo}/f_{\rm rep} = \omega_c l_c(1/\nu_g - 1/\nu_p)$. If one is interested in stabilization of $f_{\rm rep}$ only, it is sufficient to control just l_c.[6] From our previous expression for $f_{\rm ceo}$ we note that changes in the cavity length will have a minimal effect on $f_{\rm ceo}$, because ν_g and ν_p are only slightly modified by l_c. When the entire comb spectrum needs to be stabilized absolutely, one needs a control for the other degree of freedom, such as the pump laser power,[4] which influences ν_g and ν_p differently. Using an acousto-optic modulator in the pump beam's path to control the laser power produces a servo bandwidth of $\geq$100 kHz.

Previously, the dominant source of noise in $f_{\rm ceo}$ was attributed to power fluctuations, explained in terms of spectral shifts,[10] self-steepening, and nonlinear refraction.[11] In this Letter we report detailed experimental investigations of intensity-related dynamics in both the repetition and the carrier-envelope offset frequencies for both laser systems. We have observed, for the first time to our knowledge, an interesting sign reversal in the dependence of $f_{\rm rep}$ and $f_{\rm ceo}$ on the laser power. These dynamics are well accounted for by a corresponding shift of the laser pulse spectrum. Important mode-locking conditions can be found under which the intensity-related spectral shift is minimized, leading to minimum noise of both $f_{\rm rep}$ and $f_{\rm ceo}$. This new understanding has strong implications for the optimal use of power control for the femtosecond laser.

Frequencies $f_{\rm ceo}$ and $f_{\rm rep}$ depend on the laser power and hence on pulse peak intensity I, as

$$\frac{{\rm d}f_{\rm rep}}{{\rm d}I} = \frac{1}{l_c}\frac{{\rm d}\nu_g}{{\rm d}I},$$

$$\frac{{\rm d}f_{\rm ceo}}{{\rm d}I} = \frac{1}{2\pi}\frac{\partial\omega_c}{\partial I}\left(1 - \frac{\nu_g}{\nu_p}\right) + \frac{\omega_c}{2\pi}\frac{\nu_g}{\nu_p}\left(\frac{1}{\nu_p}\frac{{\rm d}\nu_p}{{\rm d}I} - \frac{1}{\nu_g}\frac{{\rm d}\nu_g}{{\rm d}I}\right),$$

where $\partial\omega_c/\partial I$ is the intensity-related laser spectral shift. Denoting by $\overline{n}$ ($\overline{n} = \overline{n}_0 + \overline{n}_2 I$) the average refractive index in the laser cavity leads to $\nu_g = c/[\overline{n} + \omega_c({\rm d}\overline{n}/{\rm d}\omega)_{\omega_c}]$ and $\nu_p = (c/\overline{n})$, which lead to the following equations:

$$\frac{{\rm d}f_{\rm rep}}{{\rm d}I} = -\frac{1}{l_c}\frac{{\nu_g}^2}{c}\left[\overline{n}_2 + \omega_c\left(\frac{{\rm d}\overline{n}_2}{{\rm d}\omega}\right)_{\omega_c} + c\frac{\partial\omega_c}{\partial I}\frac{\partial}{\partial\omega_c}\left(\frac{1}{\nu_g}\right)\right], \tag{1}$$

$$\frac{{\rm d}f_{\rm ceo}}{{\rm d}I} = \frac{{\omega_c}^2}{2\pi}\frac{{\nu_g}^2}{c^2}\left[\overline{n}_0\left(\frac{{\rm d}\overline{n}_2}{{\rm d}\omega}\right)_{\omega_c} - \overline{n}_2\left(\frac{{\rm d}\overline{n}_0}{{\rm d}\omega}\right)_{\omega_c}\right] + \frac{1}{2\pi}\frac{\partial\omega_c}{\partial I}\left[\left(1 - \frac{\nu_g}{\nu_p}\right) + \frac{\omega_c{\nu_g}^2}{\nu_p}\frac{\partial}{\partial\omega_c}\left(\frac{1}{\nu_g}\right) - \frac{\omega_c\nu_g}{c}\frac{\partial\overline{n}}{\partial\omega_c}\right]. \tag{2}$$

All terms except $\partial\omega_c/\partial I$ and $\partial(1/\nu_g)/\partial\omega_c$ are constants taken from the literature. The last term in Eq. (1) and the second term in brackets in Eq. (2) reveal the dependence of ${\rm d}f_{\rm rep}/{\rm d}I$ and ${\rm d}f_{\rm ceo}/{\rm d}I$ on the intensity-related spectral shift. Both equations are dominated by a term proportional to

0146-9592/03/100851-03$15.00/0

$(\partial\omega_c/\partial I)(\partial\nu_g^{-1}/\partial\omega_c)$, explaining the near coincidence in the sign change of $\mathrm{d}f_{\mathrm{rep}}/\mathrm{d}I$ and $\mathrm{d}f_{\mathrm{ceo}}/\mathrm{d}I$ with that of $\partial\omega_c/\partial I$. By experimentally measuring $\mathrm{d}f_{\mathrm{rep}}/\mathrm{d}I$ and $\partial\omega_c/\partial I$ we can uniquely calculate the spectrally related shift of $1/\nu_g$ (i.e., $\partial(1/\nu_g)/\partial\omega_c$). We then use this value to compute the intensity-related shift of f_{ceo}, which can be compared with a direct experimental measurement of $\mathrm{d}f_{\mathrm{ceo}}/\mathrm{d}I$.

The following parameters are needed for evaluation of these equations: For the 750-MHz (100-MHz) laser, the beam waist inside the Ti:s crystal is 10 μm (20 μm), the output coupler is 3% (12%), and the pulse bandwidth is ~22 nm (50 nm). We use these parameters to compute the pulse's peak intensity inside the Ti:s crystal. With a cavity-filling factor (defined as the ratio of Ti:s crystal length to the overall cavity length) of the 750-MHz laser of 0.006, the average $\bar{n}_0$ is 1.00456, and $\mathrm{d}\bar{n}_0/\mathrm{d}\omega \sim 6 \times 10^{-20}$ s. For the average $\bar{n}_2$ we take into account Gaussian beam propagation, and the effective cavity-filling factor becomes 0.0037. The average $\bar{n}_2$ is $\sim 7.3 \times 10^{-23}\ \mathrm{m}^2\ \mathrm{W}^{-1}$, and $\mathrm{d}\bar{n}_2/\mathrm{d}\omega \sim 1.2 \times 10^{-38}\ \mathrm{s\ m}^2\ \mathrm{W}^{-1}$, based on the value from Ref. 11 for Ti:s.

Illustrated in Fig. 1 are the intensity-related shifts of ω_c and f_{ceo} as the average output power of the 750-MHz laser varies. For these measurements, ω_c is taken to be the spectrally weighted center frequency. We verify that no cw components are present as the power is changed and that the pulse width remains constant. The center frequency is shown with respect to the vertical axis at the right as filled squares. The carrier-envelope offset frequency, measured with an f-to-$2f$ self-referencing interferometer,[3] is marked by filled circles. The change in sign of $\mathrm{d}f_{\mathrm{ceo}}/\mathrm{d}I$ is accompanied by a sign change of $\partial\omega_c/\partial I$, with a slight offset in the zero-crossing power given by the thermal response (see discussions below following Fig. 4). The filled circles in Fig. 2 show the corresponding change in sign of $\mathrm{d}f_{\mathrm{rep}}/\mathrm{d}I$ with respect to the laser power. These data are used for the calculation of $\partial(1/\nu_g)/\partial\omega_c$, which turns out to be negative, consistent with the fact that the linear GVD in the cavity is negative because the nonlinear contribution to the GVD is positive. We use the calculated values of $\partial(1/\nu_g)/\partial\omega_c$ to compute $\mathrm{d}f_{\mathrm{ceo}}/\mathrm{d}I$ by means of Eq. (2), shown as triangles in Fig. 2, and they are in good agreement with the directly measured data shown by open circles. Both f_{ceo} and f_{rep} data in Fig. 2 are obtained by direct frequency counting while the laser power slowly varies.

The magnitude of the dynamic response of $\mathrm{d}f_{\mathrm{ceo}}/\mathrm{d}I$, measured at three laser output powers, is shown in Fig. 3. (The measurements in these figures were carried out at different times when f_{ceo} reached a maximum at different laser powers). Two of these responses, with data represented by squares and circles, are for $\mathrm{d}f_{\mathrm{ceo}}/\mathrm{d}I > 0$. The third data set, represented by triangles, is obtained when $\mathrm{d}f_{\mathrm{ceo}}/\mathrm{d}I < 0$ at a higher laser power after the turn-around point. The amplitude response of the third set when the absolute value is not taken is shown at the bottom of the figure. At low Fourier frequencies there is a steep roll-off due to the thermal response of the Ti:s crystal. At higher Fourier frequencies the response curve of $\mathrm{d}f_{\mathrm{ceo}}/\mathrm{d}I$ is roughly flat, at least up to the measured range of 400 kHz. Whereas the fast response does change sign following $\mathrm{d}f_{\mathrm{ceo}}/\mathrm{d}I$, the sign of the thermal response is not affected by the zero crossing of $\mathrm{d}f_{\mathrm{ceo}}/\mathrm{d}I$.

Figure 4 shows the linewidth of f_{ceo} at various pulse powers for the 750-MHz laser. It is clear that the phase noise associated with the carrier-envelope offset frequency increases dramatically when the value of $\mathrm{d}f_{\mathrm{ceo}}/\mathrm{d}I$ deviates from zero and is at a minimum when $\mathrm{d}f_{\mathrm{ceo}}/\mathrm{d}I = 0$. This is easy to understand because at the zero-crossing point of $\mathrm{d}f_{\mathrm{ceo}}/\mathrm{d}I$, the f_{ceo} linewidth

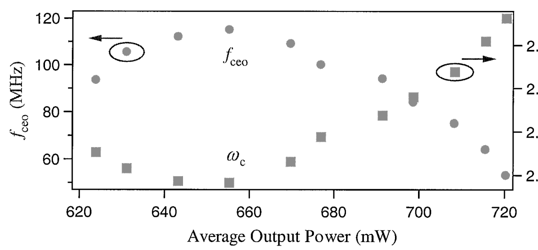

Fig. 1. Shift of ω_c and f_{ceo} with respect to the average output power from the 750-MHz laser cavity; squares, ω_c; circles, f_{ceo}.

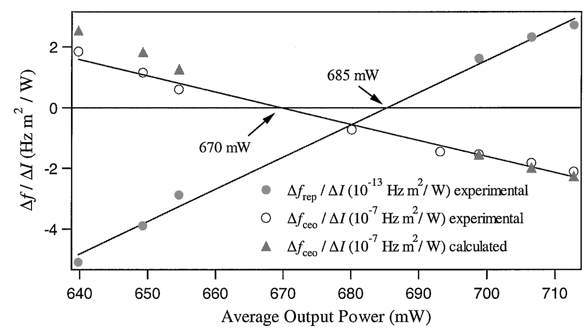

Fig. 2. Directly measured $\Delta f_{\mathrm{rep}}/\Delta I$ and $\Delta f_{\mathrm{ceo}}/\Delta I$ versus the average output power of the 750-MHz laser. Calculated $\Delta f_{\mathrm{ceo}}/\Delta I$ based on a parameter derived from the measured $\Delta f_{\mathrm{rep}}/\Delta I$ data are also shown.

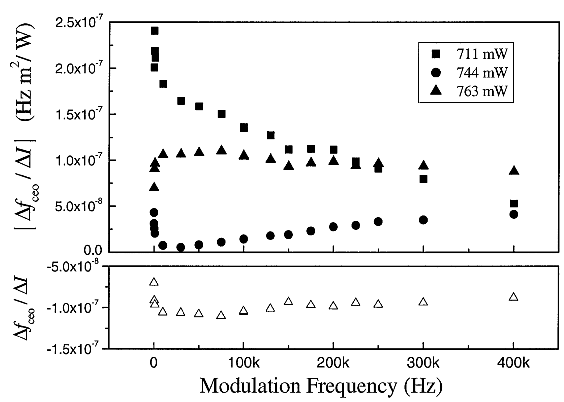

Fig. 3. Dynamic response (transfer function) of f_{ceo} with respect to the laser power for the 750-MHz laser. Notice the change of the dynamic response when f_{ceo} goes through the turning point. Bottom, the true response (inverted from the magnitude plot) for the 763-mW laser.

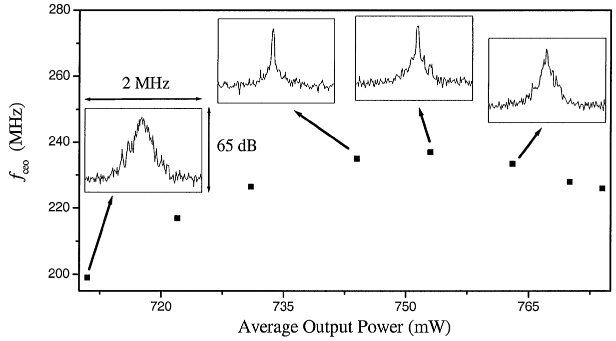

Fig. 4. Linewidth of f_{ceo} near the turning point ($\Delta f_{\text{ceo}}/\Delta I = 0$) in the 750-MHz laser.

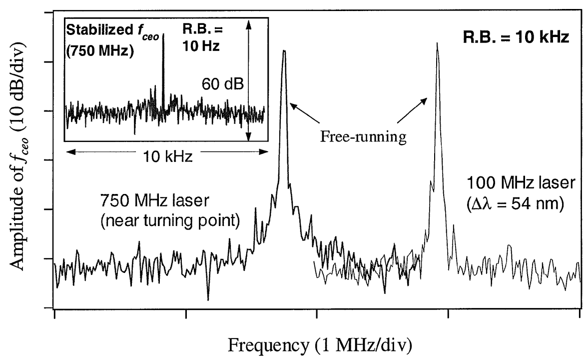

Fig. 5. Comparison of the f_{ceo} linewidths of the 100 and 750-MHz lasers. The f_{ceo} linewidth is nearly independent of the pulse intensity for the 100-MHz laser, whereas the narrowest f_{ceo} line shape is shown for the 750-MHz laser. Inset, resolution-limited linewidth of the stabilized f_{ceo} for the 750-MHz laser. R. B., resolution bandwidth.

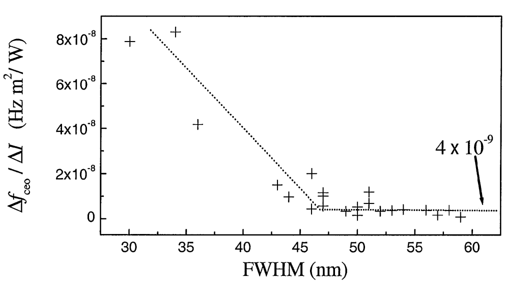

Fig. 6. Dependence of $\Delta f_{\text{ceo}}/\Delta I$ on the laser bandwidth for the 100-MHz laser.

is least sensitive to pulse intensity fluctuations, which appear to be the dominant source of noise for f_{ceo}. The narrowest linewidth does not occur exactly at the maximum value of f_{ceo} shown in the figure, which is measured at dc frequency. However, it does occur at the point where $\mathrm{d}f_{\text{ceo}}/\mathrm{d}I = 0$, as we determined by modulating the laser power at 1 kHz and using lock-in detection with the aid of a calibrated frequency-to-voltage converter. From Fig. 3 it is easy to understand that $\mathrm{d}f_{\text{ceo}}/\mathrm{d}I$ (ac measurement) should cross zero before f_{ceo} (dc measurement) reaches its maximum value, because of the thermal response at low frequencies.

In experiments that involve the stabilization of f_{ceo}, we operate the 750-MHz laser near the point where $\mathrm{d}f_{\text{ceo}}/\mathrm{d}I = 0$. Under such a condition it is possible to phase lock f_{ceo} to a highly stable radio-frequency signal and achieve a linewidth that is basically that of the radio-frequency reference. The inset of Fig. 5 shows such a stabilized f_{ceo} linewidth, which was obtained by use of a feedback loop acting on the laser pump power (bandwidth, $\approx$50 kHz). However, if $\mathrm{d}f_{\text{ceo}}/\mathrm{d}I$ is tuned away from zero, the stabilized f_{ceo} linewidth becomes increasingly larger. In sharp contrast, the 100-MHz laser shows a typical f_{ceo} linewidth that is comparable to or better than the best one for the 750-MHz laser, as shown in Fig. 5. When the pulse bandwidth of the 100 MHz laser is larger than 47 nm, the f_{ceo} linewidth is almost invariant with respect to the laser power. This can be explained by the data in Fig. 6, which shows the dependence of $\mathrm{d}f_{\text{ceo}}/\mathrm{d}I$ on the 100-MHz laser pulse bandwidth. We can observe an interesting threshold behavior: The value of $\mathrm{d}f_{\text{ceo}}/\mathrm{d}I$ decreases sharply when the pulse bandwidth increases until $\sim$47 nm; after that, $\mathrm{d}f_{\text{ceo}}/\mathrm{d}I$ remains unchanged, at a value of 4×10^{-9} Hz m^2 W^{-1}. The stronger mode-locking effect in the 100-MHz laser, which arises from the wider pulse bandwidth, allows for a smaller value of $\partial \omega_c/\partial I$ and subsequently for a smaller $\mathrm{d}f_{\text{ceo}}/\mathrm{d}I$ and a narrower f_{ceo} linewidth.

We thank D. Jones, J. L. Hall, and T. Fortier for their generous help and F. Kärtner, E. Ippen, and H. Haus for discussions. This research is funded by the U.S. Office of Naval Research, NASA, the National Science Foundation, and the National Institute of Standards and Technology. K. Holman is a Hertz Foundation graduate fellow. R. J. Jones is a National Research Council postdoctoral fellow. J. Ye's e-mail address is ye@jila.colorado.edu.

References

1. T. Udem, J. Reichert, R. Holzwarth, and T. W. Hänsch, Phys. Rev. Lett. **82,** 3568 (1999).
2. S. A. Diddams, D. J. Jones, J. Ye, S. T. Cundiff, J. L. Hall, J. K. Ranka, R. S. Windeler, R. Holzwarth, T. Udem, and T. W. Hänsch, Phys. Rev. Lett. **84,** 5102 (2000).
3. D. J. Jones, S. A. Diddams, J. K. Ranka, A. Stentz, R. S. Windeler, J. L. Hall, and S. T. Cundiff, Science **288,** 635 (2000).
4. A. Apolonski, A. Poppe, G. Tempea, C. Spielmann, T. Udem, R. Holzwarth, T. W. Hänsch, and F. Krausz, Phys. Rev. Lett. **85,** 740 (2000).
5. S. A. Diddams, T. Udem, J. C. Bergquist, E. A. Curtis, R. E. Drullinger, L. Hollberg, W. M. Itano, W. D. Lee, C. W. Oates, K. R. Vogel, and D. J. Wineland, Science **293,** 825 (2001).
6. J. Ye, L. S. Ma, and J. L. Hall, Phys. Rev. Lett. **87,** 270801 (2001).
7. J. D. Jost, J. L. Hall, and J. Ye, Opt. Express **10,** 515 (2002), http://opticsexpress.org.
8. R. K. Shelton, L. S. Ma, H. C. Kapteyn, M. M. Murnane, J. L. Hall, and J. Ye, Science **293,** 1286 (2001).
9. S. T. Cundiff, J. Ye, and J. L. Hall, Rev. Sci. Instrum. **72,** 3746 (2001).
10. L. Xu, C. Spielmann, A. Poppe, T. Brabec, F. Krausz, and T. W. Hänsch, Opt. Lett. **21,** 2008 (1996).
11. F. W. Helbing, G. Steinmeyer, U. Keller, R. S. Windeler, J. Stenger, and H. R. Telle, Opt. Lett. **27,** 194 (2002).